Water Resources and Industry 6 (2014) 64–80

Contents lists available at ScienceDirect

Water Resources and Industry

journal homepage: www.elsevier.com/locate/wri

Alkali treated Foumanat tea waste as an efficient adsorbent for methylene blue adsorption from aqueous solution

Azadeh Ebrahimian Pirbazari [a,b,*], Elham Saberikhah [a,b], Moslem Badrouh [a,b], Mohammad Saeed Emami [a,b]

[a] Faculty of Fouman, College of Engineering, University of Tehran, P.O. Box 43515-1155, Fouman 43516-66456, Iran
[b] Faculty of Caspian, College of Engineering, University of Tehran, P.O. Box 43841-119, Rezvanshahr 43861-56387, Iran

ARTICLE INFO

Article history:
Received 15 April 2014
Received in revised form
16 July 2014
Accepted 23 July 2014

Keywords:
Tea waste
Alkali treated
Methylene blue
Isotherm
Kinetic
Thermodynamic

ABSTRACT

The adsorption of methylene blue (MB) from aqueous solution by alkali treated Foumanat tea waste (ATFTW) from agriculture biomass was investigated. The adsorbent was characterized by Scanning Electron Microscopy (SEM), Fourier Transform-Infrared Spectroscopy (FT-IR) and nitrogen physisorption. FTIR results showed complexation and ion exchange appear to be the principle mechanism for MB adsorption. The adsorption isotherm data were fitted to Langmuir, Sips, Redlich-Peterson and Freundlich equations, and the Langmuir adsorption capacity, Q_{max} was found to be 461 mgg^{-1}. It was found that the adsorption of MB increases by increasing temperature from 303 to 323 K and the process is endothermic in nature. The removal of MB by ATFTW followed pseudo-second order reaction kinetics based on Lagergren equations. Mechanism studies indicated that the adsorption of MB on the ATFTW was mainly governed by external mass transport where particle diffusion was the rate limiting step.

* Corresponding author at: Faculty of Fouman, College of Engineering, University of Tehran, P.O. Box 43515-1155, Fouman 43516-66456, Iran. Tel.: +98 1327234927; fax: +98 1327237228.
E-mail address: aebrahimian@ut.ac.ir (A. Ebrahimian Pirbazari).

http://dx.doi.org/10.1016/j.wri.2014.07.003

1. Introduction

Saving water to save the planet and to make the future of mankind safe is what we need now. With the growth of mankind, society, science, technology our world is reaching to new high horizons but the cost which we are paying or will pay in near future is surely going to be too high. Among the consequences of this rapid growth is environmental disorder with a big pollution problem. Besides other needs the demand for water ("Water for People Water for Life" United Nations World Water Development Report UNESCO) has increased tremendously with agricultural, industrial and domestic sectors consuming 70%, 22% and 8% of the available fresh water, respectively and this has resulted in the generation of large amounts of wastewater [1–3] containing a number of pollutants. One of the important classes of the pollutants is dyes, and once they enter the water it is no longer good and sometimes difficult to treat as the dyes have a synthetic origin and a complex molecular structure which makes them more stable and difficult to be biodegraded [4–5]. Therefore, removal of dyes is an essential procedure of wastewater treatment before discharge. The methods to treat dyeing wastewater can be classified into two types: physical and chemical processes. Among all these methods, adsorption by activated carbon is the most common process for dye removal from wastewater. Although, the process is highly effective, the running costs are high with the need for regeneration after each sorption cycle [6]. This has led to the search for other potentially suitable alternative, that is more economical and equally an effective materials for dye removal by adsorption [7]. A number of investigations have shown that agricultural by-products such as clay [8], durian shell [9], Hevea brasiliensis [10], banana stalk waste [11] and mango seed kernel powder [12] have the potential of being used as low cost adsorbent for the removal of dyes in wastewater. Some of the advantages of using agricultural waste for wastewater treatment include simple technique, requires little processing, good adsorption capacity, selective of adsorption effluent, low cost, free availability and easy regeneration [13]. Besides, the exhausted adsorbents can be disposed of by burning and the heat used for steam generation [14]. However, the application of untreated agricultural or plant waste as adsorbents can also bring several problems such as low adsorption capacity, high chemical oxygen demand (COD) and biological oxygen demand (BOD) as well as total organic carbon (TOC) due to release of soluble organic compounds contained in the plant wastes [15]. Recently, comparative studies of cationic and anionic dye adsorption by agricultural solid wastes and some other low-cost adsorbents were reported [13,16–18]. Therefore, the agricultural wastes need to be treated or modified before being used as adsorbent. Alkali treatment is viewed as one of the widely employed chemical treatment techniques for surface modification of agricultural wastes for the purpose of improving its adsorption properties. Treatment of agricultural wastes with aqueous sodium hydroxide (NaOH) solutions breaks the covalent association between lignocellulose components, hydrolyzing hemicellulose and de-polymerising lignin [19]. This treatment has a substantial influence on morphological, molecular and supramolecular properties of cellulose, causing changes in crystallinity, pore structure, accessibility, stiffness, unit cell structure and orientation of fibrils in cellulosic fibers [20]. NaOH also improves mechanical and chemical properties of cellulose such as structural durability, reactivity and natural ion-exchange capacity. Treatment with NaOH removes natural fats and waxes from the cellulose fiber surfaces thus revealing chemically reactive functional groups like –OH [21]. In our previous work, we examined the use of Foumanat tea waste for methylene blue (MB) removal [22]. The objective of this work was to study the adsorption of methylene blue onto alkali treated Foumant tea waste (ATFTW). Adsorption kinetics, isotherms and thermodynamics were also evaluated and reported.

2. Materials and methods

2.1. Materials

The Foumanat tea waste was collected from Faculty of Fouman Cafeteria. The collected materials were washed several times with boiled water and finally with distilled water to remove any adhering dirt. The washed materials were then dried in the oven at 60 °C for 48 h. The dried tea waste was then

ground and sieved into a size range of 100–500 μm. Finally, the resulting product was stored in air-tight container for further use.

The methylene blue (MB) purchased from Merck (No. 115943), was selected as a representative reactive dye for this study. A stock solution of MB was prepared by dissolving 1.0 g of MB in 1 L of deionized water, and the concentrations of MB used (50–500 mg/L) were obtained by dilution of the stock solution. The pH of the solution was adjusted to the desired value by adding a small quantity of 0.01 M HCl or 0.01 M NaOH.

2.2. Preparation of adsorbent and characterization

Foumanat tea waste (FTW) was prepared as described previously. The dried FTW was treated in 0.05 M sodium hydroxide (NaOH) solution for 4 h. The sample was then washed thoroughly with distilled water until the sample was neutralized and dried in the oven at 60 °C for 24 h. Finally, the resulting adsorbent, alkali treated Foumanat tea waste (ATFTW) was stored in air-tight container for further use to adsorption experiments.

Fourier transform infrared (FTIR) analysis was applied to determine the surface functional groups, using FTIR spectroscope (FTIR-2000, Bruker), where the spectra were recorded from 4000 to 400 cm^{-1}. Surface morphology was studied using Scanning Electron Microscopy (Vegall-Tescan company). Specific surface area based on nitrogen physisorption was measured by Sibata surface area apparatus 1100. The samples were degassed at 100 °C for 2 h prior to the sorption measurement.

2.3. Adsorption procedure

Equilibrium isotherms were determined by shaking a fixed mass of ATFTW (0.5 g) with 100 mL of MB solutions with different initial concentrations (50, 100, 200, 300, 400 and 500 mg/L) in 250 mL glass Erlenmeyer's flasks at a temperature of 30 °C and pH=7. The procedure was repeated for temperatures 40 and 50 °C. Initial pH adjustments were carried out by adding either a 0.01 M hydrochloric acid or 0.01 M sodium hydroxide solution. After shaking the flasks for 120 min, the reaction mixtures were filtered through filter paper, and then the filtrates was analyzed for the remaining MB concentrations with spectrometry at the wavelength of maximum absorbance, 664 nm using a double beam UV–Vis spectrophotometer (Shimadzu, Model UV 2100, Japan).

2.4. Kinetic studies

Adsorption kinetics experiments were performed by contacting 200 mL MB solution of different initial concentrations ranging from 50 to 200 mg/L with 0.5 g ATFTW in a 500 mL-stopperred conical flask at room temperature. At fixed time intervals, the samples were taken from the solution and were analyzed.

2.5. Isotherm modeling

The non-linear forms of the Langmuir, Freundlich, Temkin, Sips and Redlich-Peterson isotherm models were used to analyze the equilibrium isotherm data [23]. The fitness of these models was evaluated by the non-linear coefficients of determination (R^2). The Matlab (version 7.3) software package was used for the computing.

The Langmuir adsorption isotherm assumes that adsorption takes place at specific homogeneous sites within the adsorbent and has found successful application for many processes of monolayer adsorption. The Langmuir isotherm can be written in the form (1)

$$q_e = (Q_{max} K_L C_e)/(1 + K_L C_e) \quad (1)$$

where q_e is the adsorbed amount of the dye, C_e is the equilibrium concentration of the dye in solution, Q_{max} is the monolayer adsorption capacity and K_L is Langmuir adsorption constant. The Freundlich isotherm is an empirical equation which assumes that the adsorption occurs on

heterogeneous surfaces. The Freundlich equation can be expressed as

$$q_e = K_L C_e^{1/n} \tag{2}$$

where K_F and $1/n$ are fitting constants which can be regarded roughly, the capacity and strength of adsorption, respectively. The Sips model is an additional empirical model which has the features of both the Langmuir and Freundlich isotherm models. As a combination of the Langmuir and Freundlich isotherm models, the Sips model contains three parameters, Q_{max}, K_s and $1/n$, which can be evaluated by fitting the experimental data. The Sips adsorption isotherm model can be written as follows:

$$q_e = (Q_{max} K_s C_e^{1/n})/(1 + K_s C_e^{1/n}) \tag{3}$$

Similar to the Sips isotherm, Redlich and Peterson, proposed an isotherm compromising the features of the Langmuir and the Freundlich isotherms:

$$q_e = K_{rp} C_e/(1 + \alpha_{rp} C_e^{\beta}) \lim_{x \to \infty} \tag{4}$$

In which K_{rp} and α_{rp} are the Redlich-Peterson constants, and β is basically in the range of zero to one. If β is equal to 1, The equation reduces to the Langmuir isotherm equation, while in case where the value of the term $\alpha_{rp} C_e^{\beta}$ is much bigger than one, the Redlich-Peterson isotherm equation can be approximated by a Freundlich-type equation.

Temkin isotherm was first developed by Temkin and Pyzhevand it is based on the assumption that the heat of adsorption would decrease linearly with the increase of coverage of adsorbent:

$$q_e = RT \ln(a_t C_e)/b_t \tag{5}$$

In which R is the gas constant, T the absolute temperature in Kelvin, b_t the constant related to the heat of adsorption and a_t is the Temkin isotherm constant. Temkin isotherm equation has been applied to describe adsorption on heterogeneous surface.

2.6. Kinetic models

The Lagergren rate equation [24] is one of the most widely used adsorption rate equations for the adsorption of solute from a liquid solution. The pseudo-first-order kinetic model of Lagergren may be represented by

$$dq/q_e - q = k_1 dt \tag{6}$$

Integrating this equation for the boundary conditions $t=0$ to $t=t$ and $q=0$ to $q=q_t$, gives

$$\ln(q_e - q_t) = \ln qe - k_1 t \tag{7}$$

where q_e and q_t are the amounts of adsorbate (mg/g) at equilibrium and at time t (min), respectively, and k_1 is the rate constant of pseudo-first-order adsorption (min^{-1}). The validity of the model can be checked by linearized plot of $\ln(q_e - q_t)$ vs t. Also, the rate constant of pseudo-first-order adsorption is determined from the slope of the plot.

The pseudo-second-order equation based on adsorption equilibrium capacity can be expressed as

$$dq/(q_e - q_t)^2 = k_2 dt \tag{8}$$

Taking into account, the boundary conditions $t=0$ to $t=t$ and $q=0$ to $q=q_t$, the integrated linear form the above equation can be rearranged to follow equation:

$$1/(q_e - q_t) - 1/q_e = k_2 t \tag{9}$$

Rearranging the variables gives the following equation

$$t/q_t = 1/k_2 q_e^2 + t/q_e \tag{10}$$

where the theoretical equilibrium adsorption capacity (q_e) and the second-order constants k_2 ($g\ mg^{-1}\ min^{-1}$) can be determined experimentally from the slope and intercept of plot t/q vs t.

2.7. Statistical analysis

All experiments were performed in duplicate and the mean values were presented. The data were analyzed by one-way analysis of variance (ANOVA) using SPSS 11.5 for Windows. The data was considered statistically different from control at $P < 0.05$.

2.8. Studies on point of zero charge (pH_{pzc})

In pH_{pzc} determination, 0.01 M NaCl was prepared and its pH was adjusted in the range of 2–11 by adding 0.01 M NaOH or HCl. Then, 50 mL of 0.01 M NaCl each was put in conical flask and then 0.1 g of the ATFTW was added to these solutions. These flasks were kept for 72 h and final pH of the solution was measured by using pH meter. Graphs were then plotted for pH_{final} vs $pH_{initial}$.

3. Results and discussion

3.1. FTIR spectral analysis

A closer insight into the biomass surface properties was obtained by comparing the FTIR spectra of FTW before and after alkali treatment and after MB adsorption (Fig. 1) in the range of 400–4000 cm^{-1}. FTIR spectra of ATFTW before and after adsorption of MB are shown in Fig. 1. In ATFTW spectrum before adsorption (Fig. 1b), the broad absorption peaks at around 3432 cm^{-1} correspond to the O–H stretching vibrations due to inter- and intra-molecular hydrogen bonding of polymeric compounds (macromolecular associations), such as alcohols, phenols and carboxylic acids, as in pectin, cellulose and lignin, thus, showing the presence of "free" hydroxyl groups on the adsorbent surface [25]. The peak at 2921 cm^{-1} is attributed to the symmetric and asymmetric C–H stretching vibration of aliphatic acids [25]. The peak at 1638 cm^{-1} is due to asymmetric stretching vibrations of C=O and the peak observed at 1525 cm^{-1} can be assigned to aromatic compound group. The other prominent peaks are due to NH_2 and C=O (1457 and 1046 cm^{-1}, respectively) groups.

However, in the case of ATFTW (Fig. 1(c)) after adsorption, there is remarkable shift in positions of –OH, C=O and –C–C– group peaks which indicates MB binding mostly at –OH and C=O groups. Moreover, it can be seen that some of the absolute values of ATFTW were larger than those of FTW (Fig. 1a), which indicates that ATFTW has higher physical stability and surface activity. The changes in FTIR spectra confirm the complexation of MB with functional groups present in the adsorbents. These observation also reported by Nasuha and Hameed [26].

3.2. SEM and BET analysis

SEM microghraphs of FTW and ATFTW with two magnifications are shown in Fig. 2. These results revealed that their surface morphologies were obviously different. FTW consisted of fibers with open stomata (Fig. 2a); ATFTW consisted of fibers with significant pore and uneven surface structure (Fig. 2b), which indicated that the surface area of FTW was increased for alkali treatment and the surface of ATFTW was rougher than that of FTW. This surface characteristic will substantiate the higher adsorption capacity. The surface areas of FTW and ATFTW are observed to be 21 and 45 m^2/g by BET method, respectively.

3.3. Effect of initial concentration and contact time on MB adsorption

Fig. 3 shows the effect of the initial dye concentration (50–200 mg/L) on the adsorption of MB. It was observed that amount of MB adsorbed was rapid for the first 10 min and thereafter it proceeded at a slower rate (10–80 min) and finally reached saturation. The equilibrium adsorption increases from 15.2 to 62.2 mg/g, with increase in the initial MB concentration from 50 to 200 mg/L. The findings are because as the initial concentration increases, the mass transfer driving force becomes larger, hence

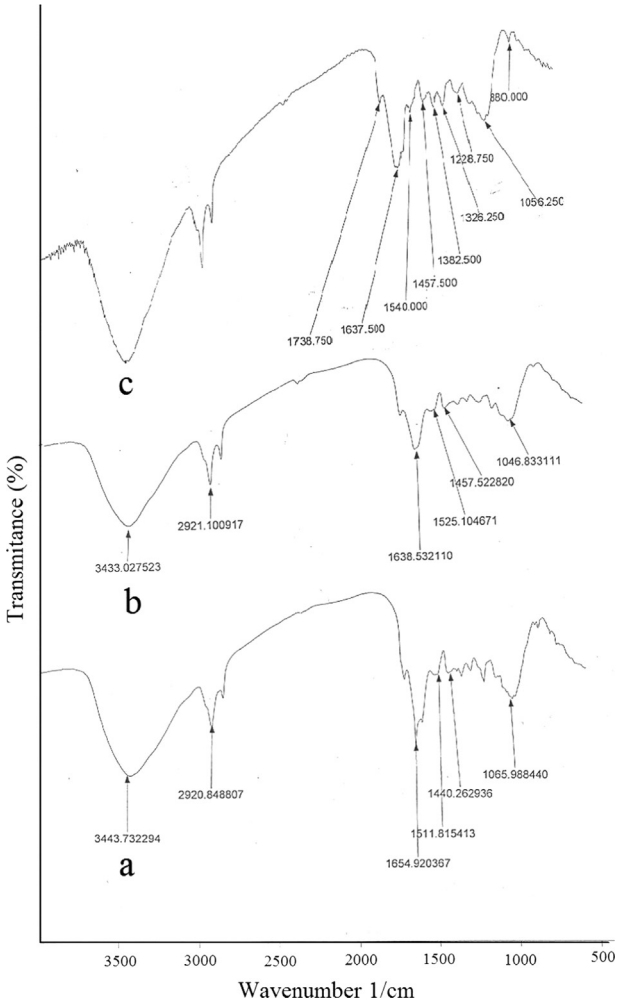

Fig. 1. FTIR spectra of (a) FTW, (b) ATFTW and (c) ATFTW after MB adsorption.

resulting in higher MB adsorption [27]. It is also shown in Fig. 3 that the contact time needed for MB solutions with initial concentrations of 50–200 mg/L to reach equilibrium was 80 min. The initial concentration provides an important driving force to overcome all mass transfer resistances of the MB between the aqueous and solid phase. However, the experimental data were measured at 120 min to be sure that full equilibrium was attained.

3.4. Effect of temperature on MB adsorption

The effect of temperature on the adsorption rate of MB on ATFTW was investigated at three different temperatures (30, 40, and 50 °C) using initial concentration of 50–500 mg/L (Fig. 4). The major effect of temperature is influence by the diffusion rate of adsorbate molecules and internal pores of the adsorbent particle. It is observed that the removal percentage of MB increases with increased temperature at all concentrations studied. An increase of temperature increases the rate of diffusion of the adsorbate molecules across the external boundary layer and within the internal

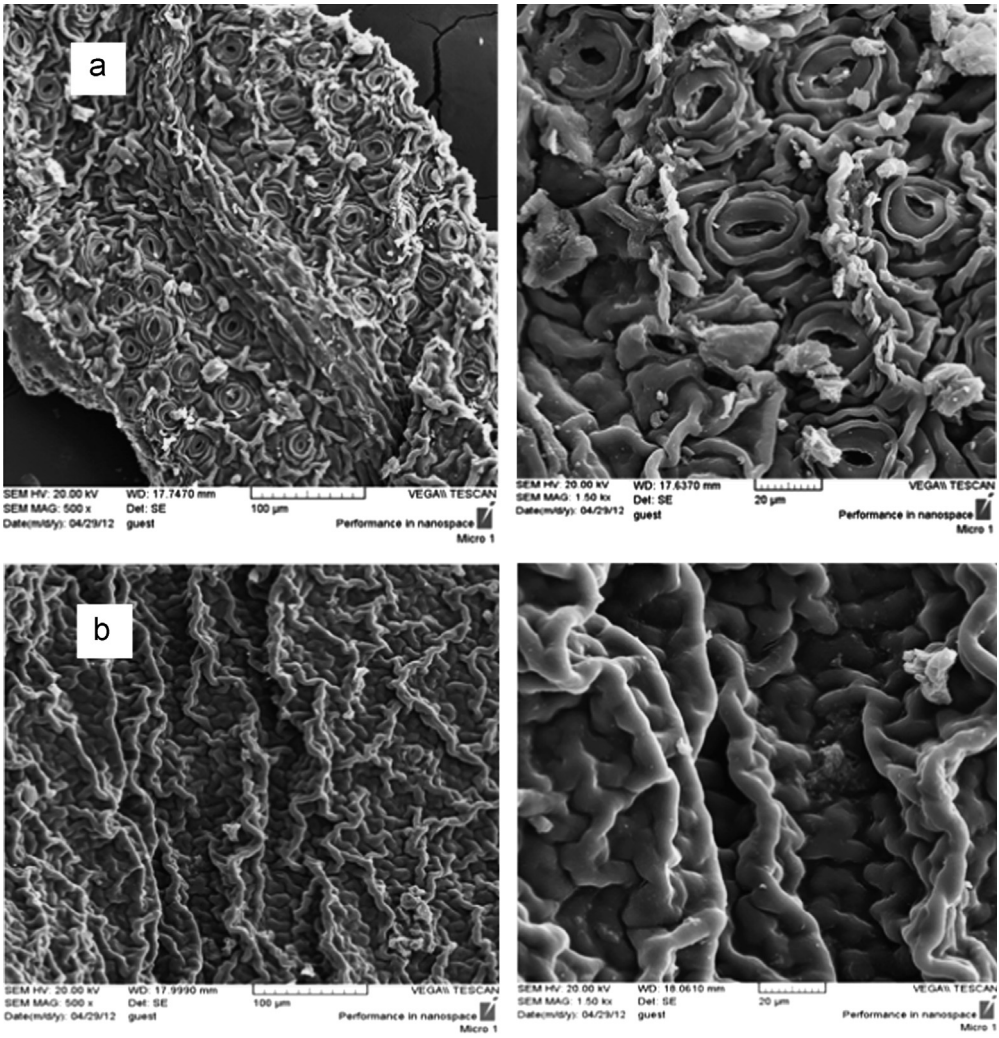

Fig. 2. SEM micrographs of (a) FTW and (b) ATFTW.

pores of the adsorbent particle, due to decrease in the viscosity of the solution [28]. From the result, an increase in temperature from 30 to 40 °C increased the ATFTW monolayer adsorption capacities from 404 to 461 mgg^{-1} (Table 1). This phenomenon indicates that the adsorption process is endothermic in nature. This may be due to the mobility of molecules which increases generally with a rise in temperature, thereby facilitating the formation of surface monolayers [29].

3.5. Point of zero charge (pH_{zpc}) studies and the effect of pH on MB adsorption

The point of zero charge (pH_{pzc}) is an important factor that determines the linear range of pH sensitivity and then indicates the type of surface active centers and the adsorption ability of the surface [30]. Many researchers studied the point of zero charge of adsorbents that prepared from agricultural solid wastes in order to better understand of adsorption mechanism. Cationic dye

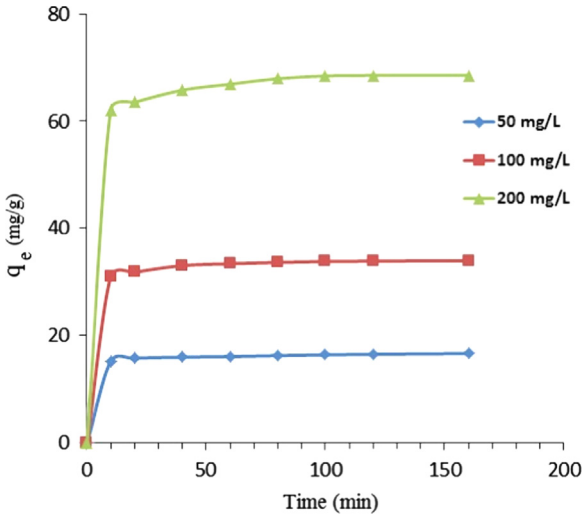

Fig. 3. Effect of contact time and initial concentration on the adsorption of MB on ATFTW.

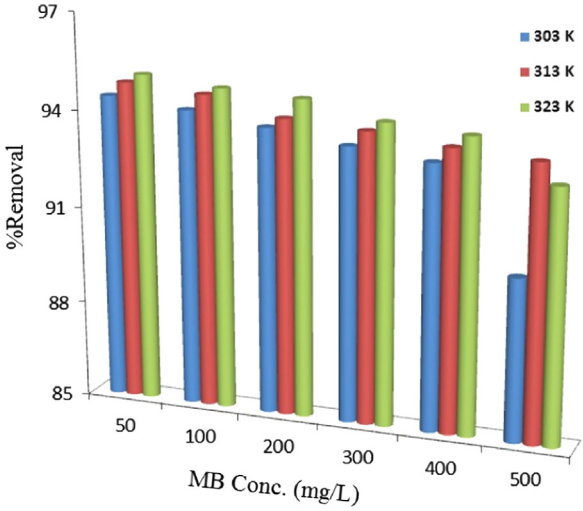

Fig. 4. Effect of temperature on the removal of MB at different initial concentrations.

adsorption is favored at pH > pH_{pzc}, due to presence of functional groups such as OH^-, COO^- groups. Anionic dye adsorption is favored at pH < pH_{pzc} where the surface becomes positively charged [31,32]. The graph of pH_{final} vs pH_{intial} was plotted as shown in Fig. 5. The intersections of the curves with the straight line are known as the end points of the pH_{pzc}, and this value is 6.7 for ATFTW. Fig. 6 shows the effect of pH on the adsorption of MB. The experiments were conducted at 250 mL of 100 mg/L initial MB concentration, 0.50 g ATFTW dose. It was observed that pH gives a significant influence to the adsorption process. MB is cationic dye, which exists in aqueous solution in the form of positively charged ions. As a charged species, the degree of its adsorption onto the adsorbent surface is primarily influenced by the surface charge on the adsorbent, which in turn is influenced by the solution pH. As shown in Fig. 6, the removal percentage was minimum at pH 2 (42%), this increased up to 6 and

Table 1
Isotherm parameters for MB adsorption by ATFTW.

Temperature (K)	303	313	323
Langmuir			
Q_{max} (mgg^{-1})	404.72	461.08	429.85
k_L (L/mg)	0.0082	0.0077	0.0089
R^2	0.9999	0.9996	0.9995
Freundlich			
n	1.16	1.14	1.15
k_F (mgg^{-1})(dm^3/mg)$^{1/n}$	4.25	4.39	4.76
R^2	0.9996	0.9999	0.9995
Temkin			
B/RT	0.0315	0.0313	0.0311
k_T (L mg^{-1})	0.3623	0.3938	0.4147
R^2	0.9095	0.9038	0.9087
Sips			
Q_{max} (mgg^{-1})	571.36	1121.5	785.87
K_s ((mg^{-1})$^{-1/n}$)	0.00637	0.00365	0.00548
$1/n$	0.9526	0.9205	0.9327
R^2	1	1	0.9997
Redlich-Peterson			
K_{rp} (L kg^{-1})	3.649	4.557	4.511
α_{rp} ($kgmg^{-1}$)	0.03947	0.151	0.08529
β	0.658	0.397	0.514
R^2	1	1	0.9997

remained nearly constant (95%) over the initial pH ranges of 6–12. This phenomenon occurred due to the presence of excess H^+ ions in the adsorbate and the negatively charged surface adsorbent. Lower adsorption of MB at acidic pH ($pH < pH_{pzc}$)is due to the presence of excess H^+ ions competing with the cation groups on the dye for adsorption sites. At higher solution pH ($pH > pH_{pzc}$), the ATFTW possibly negatively charged and enhance the positively charged dye cations through electrostatic forces of attraction. We selected pH=7 for adsorption and kinetic experiments.

3.6. Isotherm modeling

Analysis of the isotherm data is important to develop equations that correctly represent the results and could be used for design purposes. Fig. 7 and Table 1 show the fitting parameters for the measured isotherm data for MB adsorption onto ATFTW on the nonlinear forms of Langmuir, Freundlich, Temkin, Redlich-Peterson and Sips models. The values of non-linear correlation coefficients (R^2) for the Langmuir, Sips, Freundlich and Rudlich-Peterson isotherm models indicate good fit with the four models. The applicability of Langmuir, Sips and Rudlich-Peterson isotherms showed that there were effectively monolayer sorption and a homogeneous distribution of active sites on the surface of biosorbent. In all the temperatures, the Temkin isotherm represented the poorest fit of experimental data in comparison to the other isotherm equations. The value of exponent $1/n$ for the Sips model is close to unity indicating that adsorptions are rather homogeneous. The maximum MB adsorption capacity (mgg^{-1}) belongs to ATFTW as has been shown in Table 1.The monolayer capacity (Q_{max}) is 461 mgg^{-1} as calculated from Langmuir at 313 K. The Freundlich model assumes that the uptake of MB occurs on a heterogeneous adsorbent surface. The magnitude of the Freundlich constant n gives a measure of favorability of adsorption. Values of $n > 1$ represent a favorable adsorption process [33]. For the present study, the value of n also presents the same trend at all the temperatures indicating favorable nature of adsorption of MB by ATFTW.

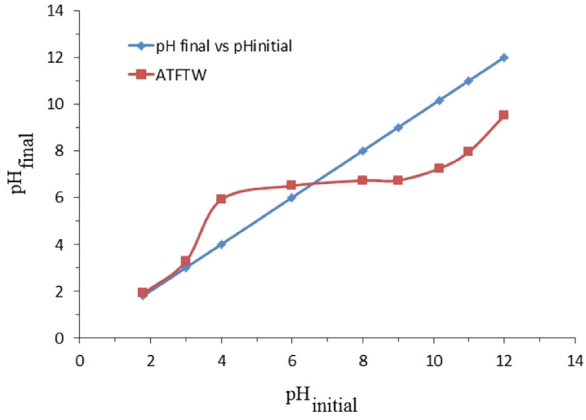

Fig. 5. Plot for determination of point of zero charge of ATFTW.

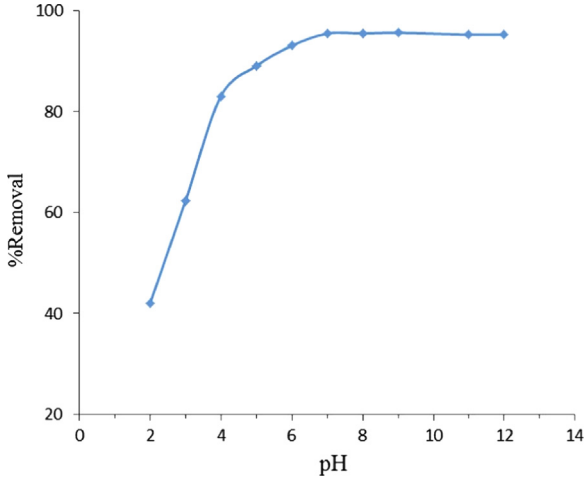

Fig. 6. Effect of solution pH on the adsorption of MB on ATFTW.

3.7. *Effect of alkali treatment of FTW on MB adsorption*

In our previous study [22], maximum saturated monolayer sorption capacity (Q_{max}) of FTW for MB was 213 mgg^{-1} at 313 K and in this study, Q_{max} of ATFTW is 461 mgg^{-1} at 313 K, suggested that carboxyl groups (–COOH) are responsible to some extent for the binding of MB cations (in aqueous solutions, MB dissociates into MB^+ and Cl^-ions). This means that increasing the number of carboxylate ligands in the biomass can enhance the binding capacity. Cellulose, pectin, hemicellulose, and lignin, which are major constituents of FTW, contain methyl esters [25] that do not bind dye significantly. However, these methyl esters can be modified to carboxylate ligands by treating the biomass with a base such as sodium hydroxide, thereby increasing the dye-binding ability of the biomass. The hydrolysis reaction of the methyl esters is as follows [34]:

$$R\text{–}COOCH_3 + NaOH \rightarrow R\text{–}COO^- + CH_3OH + Na^+ \quad (11)$$

Therefore, chemically modifying the biomass increases the number of carboxylate ligands, which can enhance the binding ability of the biomass.

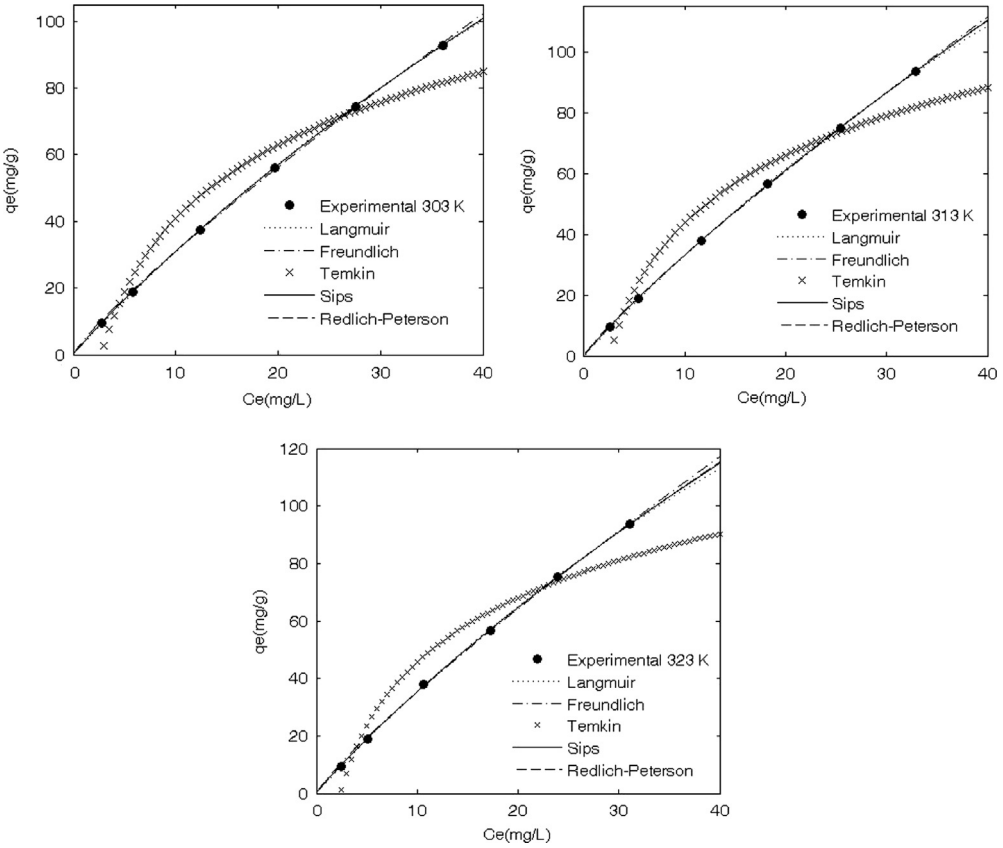

Fig. 7. Isotherm plots MB adsorption onto ATFTW at different temperatures.

3.8. Adsorption kinetics studies

The dynamics of the adsorption can be studied by the kinetics of adsorption in terms of the order of the rate constant [35]. The adsorption rate is an important factor for a better choice of material to be used as an adsorbent; where the adsorbent should have a large adsorption capacity and a fast adsorption rate. Most of adsorption studies used pseudo-first-order and pseudo-second-order models to study the adsorption kinetics. For the pseudo-first-order model, the adsorption rate was expected to be proportional to the first power of concentration, where the adsorption was characterized by diffusion through a boundary. The pseudo-first-order model sometimes does not fit well for the whole range of contact time when it failed theoretically to predict the amount of dye adsorbed and thus deviated from the theory. In that case, the pseudo-second-order equation used was based on the sorption capacity of the solid phase, where the pseudo-second-order model assumes that chemisorption may be the rate-controlling step in the adsorption processes [15,36].

The transient behavior of the MB adsorption process was analyzed by using the pseudo-first and pseudo-second-order kinetic models. Plotting ln $(q_e - q_t)$ against t permits calculation of k_1 (Fig. 8a). The rate constants, k_1, evaluated from these plots with the correlation coefficients obtained are listed in Table 2. Plotting t/q against t (Fig. 8b), gives a straight line where k_2 can be calculated. Usually the best-fit model can be selected based on the linear regression correlation coefficient R^2 values. Generally the kinetic adsorption is better represented by pseudo-second-order model for anionic and cationic dye adsorption. Lakshmi et al. [37] evaluated the adsorption of Indigo carmine dye by rice husk ash. They found that the values of the pseudo-first-order rate constant increases from 0.0087 to

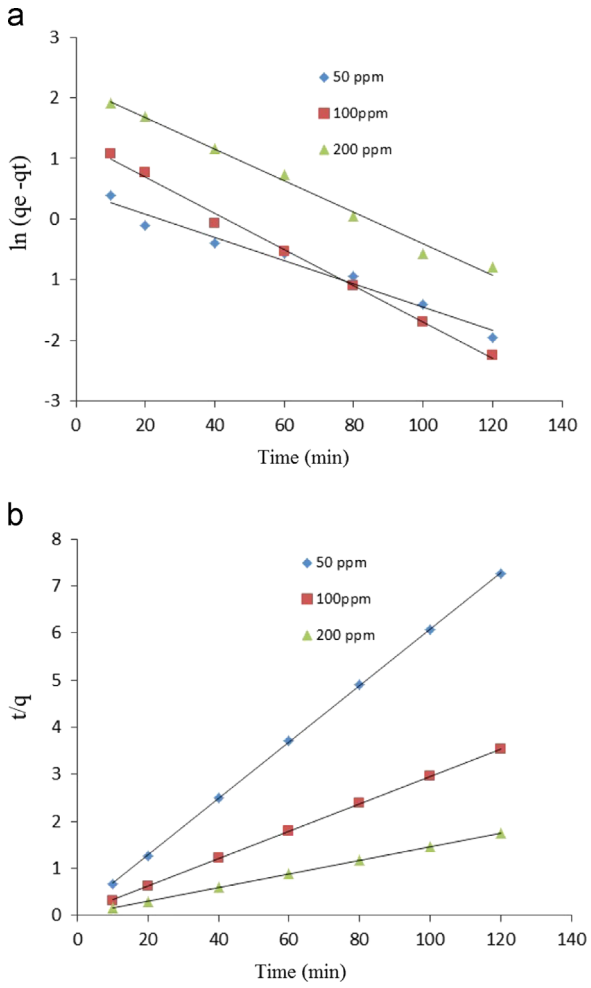

Fig. 8. Kinetic models for adsorption of MB onto ATFTW. (a) Pseudo-first-order and (b) pseudo-second-order rate equations.

Table 2
Kinetic parameters for the adsorption of MB onto ATFTW based on Lagergren rate equation.

C_0 (mg/L)	Pseudo-first order			Pseudo-second order		
	q_e(mg/g)	k_1 (1/min)	R^2	q_e (mg/g)	k_2 (g/mg min)	R^2
50	1.61	0.019	0.973	16.66	0.044	0.999
100	3.65	0.030	0.995	34.25	0.022	1.00
200	8.98	0.026	0.991	69.44	0.012	0.999

0.0122 min^{-1} with an increasing initial dye concentration from 50 to 500 mg/L, which indicates that the adsorption rate increases with an increase in initial dye concentration while the R^2 values were closer to unity for the pseudo-second-order model than that for the pseudo-first-order model. Ponnusami et al. [38] studied the use of guava leaf powder for adsorption of methylene blue. They found that the values of R^2 of the pseudo-first-order model were between 0.70 and 0.85, while the values of R^2 for the second order model were 0.999, indicating the conformity of second order model.

The R^2 listed (in Table 2) for the pseudo-first-order kinetic model was between 0.973 and 0.995. The R^2 values for pseudo-second-order model were >0.999, which is higher than the R^2 values obtained for the pseudo-first-order model. Therefore, the adsorption kinetics could well be satisfactorily more favorably described by pseudo-second-order kinetic model for MB adsorption onto ATFTW.

3.9. Adsorption mechanism

In adsorption process of dye ion on the solid surface, the dye species migrate towards the surface of the adsorbent. This type of migration proceeds till the concentration of the adsorbate species, adsorbed, on to the surface of the adsorbent. Once equilibrium is attained, the migration of the solute species from the solution stops. Under this situation, it is possible to measure the magnitude of the distribution of the solute species between the liquid and solid phases. The magnitude of this kind of distribution is a measure of the efficiency of the chosen adsorbent in the adsorbate species. When a powdered solid adsorbent material is made in contact with a solution containing dyes, the dyes first migrate from the bulk solution to the surface of the liquid film. This surface exerts a diffusion barrier. This barrier may be very significant or less significant [39]. The involvement of a significant quantum of diffusion barrier indicates the dominant role taken up by the film diffusion in the adsorption process. Furthermore, the rate of an adsorption process is controlled either by external diffusion, internal diffusion or by both types of diffusions. The external diffusion controls the migration of the solute species from the solution to the boundary layer of the liquid phase. However, the internal diffusion controls the transfer of the solute species from the external surface of the adsorbent to the internal surface of the pores of the adsorbent material [40]. It is now well established, that during the adsorption of dye over a porous adsorbent, the following three consecutive steps were taken place [41]:

(i) Transport of the ingoing adsorbate ions to external surface of the adsorbent (film diffusion).
(ii) Transport of the adsorbate ions within the pores of the adsorbent except for a small amount of adsorption, which occurs on the external surface (particle diffusion).
(iii) Adsorption of the ingoing adsorbate ions on the interior surface of the adsorbent [42].

Out of these three processes, the third process is considered to be very fast and is not the rate limiting step in the uptake of organic compounds. The remaining two steps impart the following three possibilities:

Case 1 External transport > internal transport, where rate is governed by particle diffusion.
Case 2 External transport < internal transport, where the rate is governed by film diffusion.
Case 3 External transport ≈ internal transport, which accounts for the transport of the adsorbate ions to the boundary and may not be possible within a significant rate, which later on gives rise to the formation of a liquid film surrounded by the adsorbent particles with a proper concentration gradient.

In order to predict the actual slow step involved in the adsorption process, the kinetic data were further analyzed using the Boyd model given by Eq. (12) [43]

$$B_t = -0.4977 - \ln(1-F) \tag{12}$$

F represents the fraction of solute adsorbed at any time, t (h), as calculated using Eq. (13)

$$F = q_t/q_e \tag{13}$$

where q_t and q_e are amounts adsorbed after time t and after infinite time (160 min), respectively. The calculated B_t values were plotted against time $t(h)$, as shown in Fig. 9. The plot of B_t vs time

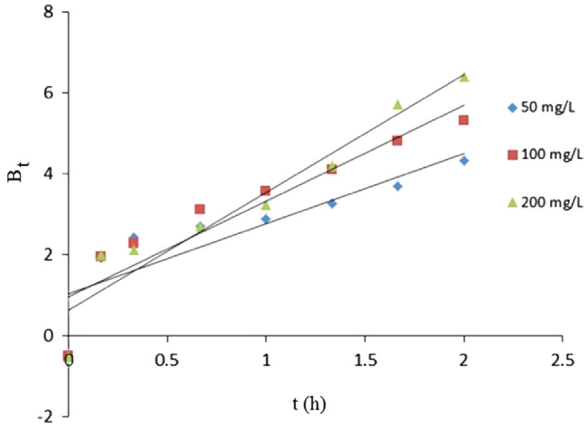

Fig. 9. Plot of B_t vs time for different initial concentrations of MB.

distinguishes between the film-diffusion and particle-diffusion-controlled rates of adsorption. The linear lines for all MB initial concentrations did no pass through the origin and the points were scatterd. This indicated that the adsorption of MB on the ATFTW was mainly governed by external mass transport where particle diffusion was the rate limiting step [43].

3.10. Adsorption thermodynamics

In environmental engineering practice, both energy and entropy factors must be considered in order to determine what processes will occur spontaneously [44]. Gibb's free energy change, ΔG^0, is the fundamental criterion of spontaneity. Reactions occur spontaneously at a given temperature if ΔG^0 is a negative value. The thermodynamic parameters of ΔG^0, enthalpy change, ΔH^0, and entropy change, ΔS^0, for the adsorption processes are calculated using the following equations [44,45].

$$\Delta G^0 = -RT \ln K_D \tag{14}$$

K_D, is given by the following equation:

$$K_D = q_e/C_e \tag{15}$$

where K_D is the distribution coefficient [45] and

$$\ln K_D = -\Delta H^0/R(1/T) + \Delta S^0/R \tag{16}$$

where R is universal gas constant (8.314 J/mol K) and T is the absolute temperature in K. A plot of ln K_D vs $1/T$ was found to be linear (Fig. 10). The values of ΔH^0 and ΔS^0 were respectively determined from the slope and intercept of the plot. The thermodynamic parameter, ΔG^0, is shown in Table 3. ΔH^0 and ΔS^0 for the sorption process were calculated to be +6.312 kJ/mol and +28.55 J/mol K, respectively. The negative value of ΔG^0 confirms the feasibility of the process and the spontaneous nature of sorption with a high preference for MB to sorb onto ATFTW. The value of ΔH^0 was positive, indicating that the sorption reaction is endothermic. The positive value of ΔS^0 (Table 3) shows that the freedom of MB is not too restricted in ATFTW confirming a physical adsorption, which is further confirmed by the relatively low values of ΔG^0.

The activation energy (E_a) was obtained from the slope of plot ln $(1-\theta)$ against $1/T$, where the surface coverage (θ) was calculated from the relation Eq. (17) [45,46].

$$\theta = 1 - C/C_0 \tag{17}$$

where C_0 and C are the initial and residual concentration of MB in solution, respectively (mg/L).

In order to further support the assertion that physical adsorption is the predominant mechanism, the values of sticking probability (S^*) was estimated from the experimental data. It was calculated

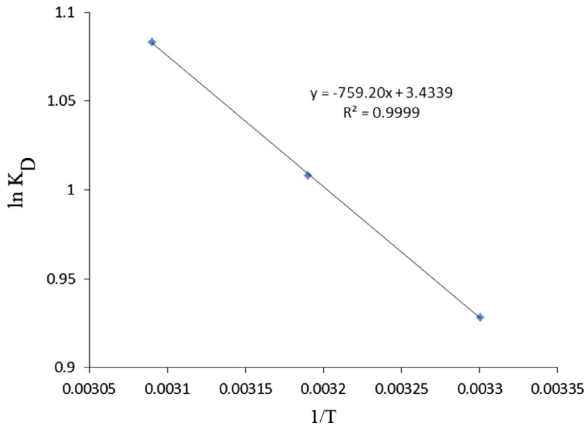

Fig. 10. Plot of ln K_D vs $1/T$ for initial concentration of MB (500 mg/L).

Table 3
Thermodynamic parameters for the adsorption of MB onto ATFTW.

Langmuir-1 isotherm					
Temperature (K)	ΔG^0 (kJ/mol)	ΔH^0 (kJ/mol)	ΔS^0 (J/mol K)	E_a (kJ/mol)	S^*
303	−2.238	+6.312	+28.55	+0.04	1
313	−2.684				
323	−2.951				

S^*: sticking probability.

using a modified Arrhenius type equation related to surface coverage as expressed in Eq. (18) [45,47].

$$S^* = (1-\theta)e_a^{-(E/RT)} \tag{18}$$

The parameter S^* indicates the measure of the potential of an adsorbate to remain on the adsorbent indefinitely. It can be expressed as in Table 3. The effect of temperature on the sticking probability was evaluated throughout the temperature range from 303 to 323 K by calculating the surface coverage at the various temperatures. The apparent activation energy (E_a) and the sticking probability (S^*) are estimated from the plot with reasonable good fit for the MB on ATFTW. The E_a values calculated from the slope of the plot were found to be 0.04 kJ/mol. The positive values of E_a indicate that higher solution temperatures favors MB removal by adsorption onto ATFTW and the adsorption process is endothermic in nature. Relatively low values of E_a suggest that MB adsorption is a diffusion controlled process. The results as shown in Table 3 indicate that the probability of MB sticking to the ATFTW surface is $S^*=1$ for MB (Table 3). This value confirms that, the sorption process is linear sticking relationship between adsorbate and adsorbent, possible mixture of physisorption and chemisorption mechanism [47].

3.11. Comparison with other bioadsorbents

A comparison of the maximum adsorption capacity (Q_{max} value) of ATFTW with those of other low-cost adsorbents in the literatures is shown in Table 4. The ATFTW shows the comparable adsorption capacity for MB with respect to other low-cost adsorbents. However, the adsorption capacity was higher than those of other adsorbents. Therefore, ATFTW was suitable and promising for MB removal from aqueous solutions since it has a relatively high adsorption capacity.

Table 4
Comparison of the Q_{max} based on Langmuir isotherm of MB on various adsorbents.

Adsorbent	Q_{max} (mgg^{-1})	References
ATFTW	461	This work
Foumant tea waste	244	[22]
NaOH-modified rejected tea	242.11	[26]
Wheat straw	57.2	[48]
Carboxymethylation wheat straw	266.7	[48]
Citric acid treated wheat straw	432.8	[49]
Modified rice straw	208.33	[50]
NaOH-treated raw kaolin	16.34	[51]
NaOH-treated pure kaolin	20.49	[51]
Tea waste	85.5	[52]

4. Conclusion

The efficiency of alkali treated Foumanat tea waste (ATFTW) in removing methylene blue dye from aqueous solution has been investigated. Results indicate that adsorption is positively dependent on temperature. The adsorption isotherm data were fitted to Langmuir, Sips, Redlich-Peterson and Freundlich isotherms. The adsorption capacity was found to be 461 mgg^{-1} at 313 K. The kinetics of adsorption followed pseudo-second order kinetics. The removal efficiency increases with the increase in temperature and hence adsorption process is endothermic in nature. The developed ATFTW not only has demonstrated higher adsorption efficiency and fast kinetics but also have shown additional benefits like cost-effectiveness and environmental-friendliness. It can be concluded to be a promising advanced adsorbent in environmental pollution cleanup.

Acknowledgments

The authors wish to acknowledge the financial support of the University of Tehran.

References

[1] R. Helmer, I. Hespanhol, Water Pollution Control – A Guide to the Use of Water Quality Management Principles, E & FN Spon, London, Great Britain, 1997.
[2] J.H. Lehr, T.E. Gass, J. Pettyjohn DeMarre, Domestic Water Treatment, McGraw-Hill Book Company, New York, 1980.
[3] N.L. Nemerrow, Industrial Water Pollution: Origins, Characteristics, and Treatment, Addison-Wesley Publishing Company, Massachusetts, 1978.
[4] E. Forgacs, T. Cserhati, G. Oros, Removal of synthetic dyes from wastewaters: a review, Environ. Int. 30 (2004) 953–971.
[5] H.S. Rai, M.S. Bhattacharyya, J. Singh, T.K. Bansal, P. Vats, U.C. Banerjee, Removal of dyes from the effluent of textile and dyestuff manufacturing industry: a review of emerging techniques with reference to biological treatment, Crit. Rev. Environ. Sci. Technol. 35 (2005) 219–238.
[6] T. Robinson, B. Chandran, P. Nigam, Effect of pretreatment of three waste residues, wheat straw, corncobs and barley husks on dye adsorption, Bioresour. Technol. 85 (2002) 119–124.
[7] A. Gurses, S. Karaca, C. Dogar, R. Bayrak, A. Acikyildiz, M. Yalcin, Determination of adsorptive properties of clay/water system: methylene blue sorption, J. Colloid Interface Sci. 269 (2004) 310–314.
[8] T.C. Chandra, M.M Mirna, Y. Sudaryanto, S. Ismajdi, Adsorption of basic dye onto activated carbon prepared by durian shell: studies of adsorption equilibrium and kinetic, Chem. Eng. J. 127 (2007) 121–129.
[9] B.H. Hameed, F.B.M. Daud, Adsorption studies of basic dye on activated carbon derived from agricultural waste: *Hevea brasiliensis* seed coat, Chem. Eng. J. 139 (2008) 48–55.
[10] B.H. Hameed, D.K. Mahmoud, A.L. Ahmad, Sorption equilibrium and kinetics of basic dye from aqueous solution using banana stalk waste, J. Hazard. Mater. 158 (2008) 499–506.
[11] K.V. Kumar, A. Kumaran, Removal of methylene blue by mango seed kernel powder, Biochem. Eng. J. 27 (2005) 83–93.
[12] W.S. WanNgah, M.A.K.M. Hanafiah, Removal of heavy metal ions from wastewater by chemically modified plant wastes as adsorbents: a review, Bioresour. Technol. 99 (2008) 3935–3948.
[13] V.K. Gupta, Suhas, Application of low-cost adsorbents for dye removal – a review, J. Environ. Manag. 90 (2009) 2313–2342.
[14] I. Gaballah, D. Goy, E. Allain, G. Kilbertus, J. Thauront, Recovery of copper through decontamination of synthetic solutions using modified barks, Metall. Mater. Trans. B 28 (1997) 13–23.
[15] G. Crini, P.M. Badot, Application of chitosan, a natural amino polysaccharide, for dye removal from aqueous solutions by adsorption processes using batch studies: a review of recent literature, Prog. Polym. Sci. 33 (2008) 399–447.

[16] M.A. Mohammed, A. Shitu, A. Ibrahim, Removal of methylene blue using low cost adsorbent: a review, Res. J. Chem. Sci. 4 (2014) 91–102.
[17] M.A. Oladipo, I.A. Bello, D.O. Adeoye, K.A. Abdulsalam, A.A. Giwa, Sorptive removal of dyes from aqueous solution: a review, Adv. Environ. Biol. 7 (2013) 3311–3327.
[18] M.A. Mohd Salleh, D. Khalid Mahmoud, W.A. Wan Abdul Karim, A. Idris, Cationic and anionic dye adsorption by agricultural solid wastes: a comprehensive review, Desalination 280 (2011) 1–13.
[19] J. Vadiveloo, B. Nurfariza, J.G. Fadel, Nutritional improvement of rice husks, Anim. Feed Sci. Technol. 151 (2009) 299–305.
[20] J. Siroky, R.S. Blackburn, T. Bechtold, J. Taylor, P. White, Alkali treatment of cellulose II fibers and effect on dye sorption, Carbohydr. Polym. 84 (2011) 299–307.
[21] B.S. Ndazi, S. Karlsson, J.V. Tesha, C.W. Nyahumwa, Chemical and physical modifications of rice husks for use as composite panels, Compos. Part A: Appl. Sci. Manuf. 38 (2007) 925–935.
[22] A. Ebrahimian, E. Saberikhah, Biosorption of methylene blue onto Foumant tea waste: equilibrium and thermodynamic studies, Cellul. Chem. Technol. 47 (2013) 657–666.
[23] Y. Liu, Y.J. Liu, Biosorption isotherms, kinetics and thermodynamics, Sep. Purif. Technol. 61 (2008) 229–242.
[24] S. Lagergren, About the theory of so-called adsorption of soluble substances, K. Sven. Vetenskapsakad. Handl. 24 (1898) 1–39. (1898).
[25] R. Gnanasambandam, A. Protor, Determination of pectin degree of esterification by diffuse reflectance Fourier transform infrared spectroscopy, Food Chem. 68 (2000) 327–332.
[26] N. Nasuha, B.H. Hameed, Adsorption of methylene blue from aqueous solution onto NaOH-modified rejected tea, Chem. Eng. J. 166 (2011) 783–786.
[27] N. Nasuha, B.H. Hameed, Azam T. Mohd Din, Rejected tea as a potential low-cost adsorbent for the removal of methylene blue, J. Hazard. Mater. 175 (2010) 126–132.
[28] J. Ghasemi, S. Asadpour, Thermodynamics' study of the adsorption process of methylene blue on activated carbon at different ionic strengths, J. Chem. Thermodyn. 39 (2007) 967–971.
[29] M. Dogan, M. Alkan, Adsorption kinetics of methyl violet onto perlite, Chemosphere 50 (2003) 517–528.
[30] A.A. Poghossian, Determination of the pH_{pzc} of insulators surface from capacitance–voltage characteristics of MIS and EIS structures, Sens. Actuator B: Chem. 44 (1997) 551–553.
[31] L.R. Radovic, I.F. Silva, J.I. Ume, J.A. Menendez, C.A. Leon, Y.A.W. Leon, A.W. Scaroni, An experimental and theoretical study of the adsorption of aromatics possessing electron-withdrawing and electron-donating functional groups by chemically modified activated carbons, Carbon 35 (1997) 1339–1348.
[32] D. Savova, N. Petrov, M.F. Yardim, E. Ekinci, T. Budinova, M. Razvigorova, V. Minkova, The influence of the texture and surface properties of carbon adsorbents obtained from biomass products on the adsorption of manganese ions from aqueous solution, Carbon 41 (2003) 1897–1903.
[33] S. Chakraborty, S. Chowdhury, P.D. Saha, Adsorption of Crystal Violet from aqueous solution onto NaOH-modified rice husk, Carbohydr. Polym. 86 (2011) 1533–1541.
[34] F. Ning-chuan, G. Xue-yi, L. Sha, Enhanced $Cu(^{2+})$ adsorption by orange peel modified with sodium hydroxide, Trans. Nonferr. Met. Soc. China 20 (2010) s146–s152.
[35] V. Gómez, M.S. Larrechi, M.P. Callao, Kinetic and adsorption study of acid dye removal using activated carbon, Chemosphere 69 (2007) 1151–1158.
[36] Z. Aksu, Application of biosorption for the removal of organic pollutants: a review, Proc. Biochem. 40 (2005) 997–1026.
[37] U.R. Lakshmi, V.C. Srivastava, I.D. Mall, D.H. Lataye, Rice husk ash as an effective adsorbent: evaluation of adsorptive characteristics for Indigo Carmine dye, J. Environ. Manag. 90 (2009) 710–720.
[38] V. Ponnusami, S. Vikram, S.N. Srivastava, Guava (*Psidium guajava*) leaf powder: novel adsorbent for removal of methylene blue from aqueous solutions, J. Hazard. Mater. 152 (2008) 276–286.
[39] V.K. Gupta, A. Mittal, V. Gajbe, Adsorption and desorption studies of a water soluble dye, Quinoline Yellow, using waste materials, J. Colloid Interface Sci. 284 (2005) 89–98.
[40] V.K. Gupta, I. Ali, D. Suhas, Mohan, Equilibrium uptake and sorption dynamics for the removal of a basic dye (basic red) using low-cost adsorbents, J. Colloid Interface Sci. 265 (2003) 257–264.
[41] J. Crank, The Mathematics of Diffusion, 2nd ed., Clarendon, Oxford, 1975.
[42] W.J. Weber, J.C. Morris, Kinetics of adsorption on carbon from solution, J. Sanit. Eng. Div. 89 (1963) 31–60.
[43] I.A.W. Tan, B.H. Hameed, Adsorption isotherms, thermodynamics and desorption studies of basic dye on activated carbon derived from oil palm empty fruit bunch, J. Appl. Sci. 10 (2010) 2565–2571.
[44] Y.S. Ho, Isotherms for the sorption of lead onto peat: comparison of linear and non-linear methods, Pol. J. Environ. Stud. 15 (2006) 81–86.
[45] H-J. Butt, K. Graf, M. Kappl, Physics and Chemistry of Interfaces, WILEY-VCH Verlag GmbH & Co.KGaA, Weinheim, 2003 (Chapter 9).
[46] L. Bulgariu, M. Răţoi, D. Bulgariu, M. Macoveanu, Equilibrium study of Pb(II) and Hg(II) sorption from aqueous solution by moss peat, Environ. Eng. Manag. J. 7 (2008) 511–516.
[47] Jnr. M. Horsfall, A.I. Spiff, Effects of temperature on the sorption of Pb^{2+} and Cd^{2+} from aqueous, Electron. J. Biotechnol. 8 (2005) 162–169.
[48] W. Zhang, H. Yan, H. Li, Z. Jiang, L. Dong, X. Kan, H. Yang, A. Li, R. Cheng, Removal of dyes from aqueous solutions by straw based adsorbents: batch and column studies, Chem. Eng. J. 168 (2011) 1120–1127.
[49] R. Han, L. Zhang, C. Song, M. Zhang, H. Zhu, L. Zhang, Characterization of modified wheat straw, kinetic and equilibrium study about copper ion and methylene blue adsorption in batch mode, Carbohydr. Polym. 79 (2010) 1140–1149.
[50] R. Gong, Y. Jin, J. Chen, Y. Hu, J. Sun, Removal of basic dyes from aqueous solution by sorption on phosphoric acid modified rice straw, Dyes Pigments 73 (2007) 332–337.
[51] D. Ghosh, K.G. Bhattacharyya, Adsorption of methylene blue on kaolinite, Appl. Clay Sci. 20 (2002) 295–300.
[52] Md. T. Uddin, Md.A. Islam, S. Mahmud, Md. Rukanuzzaman, Adsorptive removal of methylene blue by tea waste, J. Hazard. Mater. 164 (2009) 53–60.